

Supporting Material for Stick-slip motion of an Antarctic Ice Stream: the effects of viscoelasticity

Daniel Goldberg
Christian Schoof
Olga Sergienko

May 29, 2014

1 Asymptotically accurate description of stick-slip cycle

1.1 The model

A simplified version of the model in the paper, ignoring longitudinal stresses and coupling with the grounding line (i.e. $L \rightarrow \infty$) and allowing only for a driving stress τ_d , is

$$\frac{\partial(H\tau_{xy})}{\partial y} - \tau_b = \tau_d \quad (1)$$

where τ_d , considered to be constant in y , may depend on time t . For simplicity, we further restrict ourselves to a linear viscoelastic rheology, equivalent to putting $n = 1$ in Glen's law:

$$\frac{\partial\tau_{xy}}{\partial t} + \nu\tau_{xy} = G\frac{\partial u}{\partial y} \quad (2)$$

or

$$T_m \frac{\partial\tau_{xy}}{\partial t} + \tau_{xy} = \eta \frac{\partial u}{\partial y} \quad (3)$$

where $T_m = \nu/G$ is known as the Maxwell time. We specify a velocity-weakening plastic rheology with a time delay as

$$\tau_b = \tau_{yld} u/|u| \quad \text{if } |u| > 0, \quad (4a)$$

$$|\tau_b| \leq \tau_{yld} \quad \text{if } u = 0, \quad (4b)$$

where

$$T_b \frac{\partial \tau_{yld}}{\partial t} + \tau_{yld} = \tau_s \{1 - \beta[1 - \exp(-|u|/u_0)]\}, \quad (5)$$

where T_b is a friction adjustment timescale, τ_s is static friction while $\beta = (\tau_s - \tau_k)/\tau_s \in (0, 1)$ is the fractional drop from static to dynamic friction, and u_0 is the velocity scale over which the adjustment from static to dynamic friction occurs.

As a regularization of the above, we can also use

$$\tau_b = \frac{\tau_c u}{\sqrt{\epsilon^2 + u^2}}$$

instead of (4) with sufficiently small $\epsilon \ll u_0$; this does not affect the asymptotic results we develop below.

As boundary conditions, we impose zero velocity at the ice stream margins $y = 0$ and W ,

$$u(0, t) = u(W, t) = 0.$$

Our analysis below describes the stick-slip cycle as a highly nonlinear, spatially extended oscillator.

1.2 Scaled model

Assume L , H and τ_0 are given. We pick scales appropriate for viscous flow, and scale time with the Maxwell time,

$$[y] = W/2, \quad \nu H [u]/[y]^2 = [\tau_b] = \tau_s, \quad [t] = T_m. \quad (6)$$

This yields the dimensionless parameters

$$\alpha = T_m/T_b, \quad \gamma = [u]/u_0, \quad (7)$$

and we define dimensionless variables as

$$y = [y]y^*, \quad t = [t]t^* \quad u = [u]u^*, \quad \tau_{xy} = ([\tau_b][y]/H)\tau^*$$

$$\tau_b = [\tau_b]\tau_b^*, \quad \tau_{yld} = [\tau_b]\tau_c^*, \quad \tau_d = -[\tau_b]f^*.$$

(note the symbol τ_d has been replaced by $-f$.)

For simplicity, we drop the asterisks immediately. In dimensionless form, the model reads

$$\frac{\partial \tau}{\partial y} - \tau_b + f = 0, \tag{8a}$$

$$\frac{\partial \tau}{\partial t} + \tau = \frac{\partial u}{\partial y}, \tag{8b}$$

$$\tau_b = \tau_c u / |u| \quad \text{if } |u| > 0, \tag{8c}$$

$$|\tau_b| \leq \tau_c \quad \text{if } u = 0, \tag{8d}$$

$$\frac{\partial \tau_c}{\partial t} = \alpha(1 - \beta[1 - \exp(-\gamma|u|)] - \tau_c), \tag{8e}$$

$$u(0, t) = u(2, t) = 0. \tag{8f}$$

We assume that the friction adjustment (or slip event) timescale T_s is fast compared with the Maxwell time, so $\alpha \gg 1$, and that the dynamic friction velocity scale u_0 is not large, so γ is not small. To be precise, we assume that γ is strictly $O(1)$, though our results actually still apply for some large γ . We also assume that the driving stress f may vary significantly on timescales comparable with T_m but not on time scales compared with the slip event time scale T_b , and also that f is constant across the width of the ice stream. Lastly, we require that $f > 1$ at least for most of the stick-slip cycle. As we will see later, $f < 1$ corresponds to a single slip event at most.

1.3 Stick-slip dynamics

Note that the drop in basal yield stress τ_c from static to dynamic friction in (8e) is essential in generating stick-slip motion. With the friction and Maxwell time scales well separated ($\alpha \gg 1$), this drop occurs over a short period of time, of length $O(1/\alpha)$ in dimensionless terms. To capture the dynamics associated with this (and hence to describe a slip event) requires a rescaling.

1.3.1 Slip events

A fast time scale on which friction adjusts can be written as

$$T = \alpha(t - t_n),$$

where t_n is the start of the n th slip event. On the fast timescale associated with T , the viscoelastic rheology of ice will be dominated by its elastic component, represented by $\partial\tau/\partial t$ in (8b). In order for sufficiently large elastic stresses to be generated in (8b) during a slip event to ensure force balance is maintained, we also require a rescaling of velocity as

$$U = u/\alpha. \quad (9)$$

In other words, velocities can be expected to be much larger than their expected ‘viscous’ values during a slip event.

With this rescaling in hand, we get

$$\frac{\partial\tau}{\partial y} - \tau_b + f = 0, \quad (10a)$$

$$\frac{\partial\tau}{\partial T} + \alpha^{-1}\tau = \frac{\partial U}{\partial x}, \quad (10b)$$

$$\tau_b = \tau_c U/|U| \quad \text{if } |U| > 0, \quad (10c)$$

$$|\tau_b| \leq \tau_c \quad \text{if } U = 0, \quad (10d)$$

$$\frac{\partial\tau_c}{\partial T} = 1 - \beta[1 - \exp(-\gamma\alpha|U|)] - \tau_c, \quad (10e)$$

$$U(0, T) = U(2, T) = 0. \quad (10f)$$

Now we can make use of the fact that $\alpha \gg 1$ to simplify the above by dropping terms of $O(\alpha^{-1})$. In addition, with $\gamma \gtrsim 1$, we can also approximate $\exp(-\gamma\alpha U) \sim 0$ (except near the margins of the ice stream, where $U \rightarrow 0$; however, as shown in §1.3.2, this does not have a leading order effect on the flow of the bulk of the ice stream). Then we have a purely elastic model with evolving dynamic friction. Assume $U > 0$ during the slip event. Then $\tau_b = \tau_c$. Owing to our assumption that f does not change significantly on the slip time scale, we can treat f as independent of T . Differentiating (10a) with respect to time and combining this with (10b) and (10e) gives

$$\frac{\partial^2 U}{\partial y^2} + \tau_c - 1 + \beta = 0 \quad (11)$$

subject to $U(0, T) = U(2, T) = 0$. In the meantime, (10e) gives

$$\frac{\partial \tau_c}{\partial T} + \tau_c = 1 - \beta. \quad (12)$$

This has solution

$$\tau_c = (1 - \beta) + [\tau_{c0} - (1 - \beta)]e^{-T}, \quad (13)$$

where $\tau_{c0}(x)$ is the yield stress at position x at the beginning of the slip event. Basal yield stress exponentially approaches its dynamic friction value of $(1 - \beta)$.

We will show shortly that the initial basal yield stress is simply its static friction value $\tau_{c0} \equiv 1$ and so does not depend on position, in which case (11) together with $U(0) = U(2) = 0$ can be solved as

$$U = \frac{[\tau_{c0} - (1 - \beta)]e^{-T}}{2} (2y - y^2). \quad (14)$$

The velocity profile maintains the same shape but its amplitude decays exponentially during the slip event, as the result of elastic stresses building up. These elastic stresses can be computed at any point in time from (10a). Using the symmetry of the system about $y = 1$, we expect from (10a) and (13) (with τ_{c0} independent of y)

$$\tau = \{(1 - \beta - f_n) + [\tau_{c0} - (1 - \beta)]e^{-T}\} (y - 1). \quad (15)$$

Here, we use f_n to denote $f(t_n)$, assuming that the driving stress may vary on the outer time scale associated with the slow time variable t , but remains constant over the slip event. Clearly, τ exponentially approaches the steady profile $(1 - \beta - f_n)(y - 1)$ required to maintain force balance at dynamic friction.

1.3.2 Termination of the slip event

As velocity decays at the same time as elastic stresses build up, we expect the slip eventually to stop altogether, so the basal yield stress τ_c can return to its static friction value. This cannot be captured by the exponential decay in (14) and (13) alone: this never leads to U actually reaching zero, and bed strength attaining static friction values as we have assumed is the case during the stick phase. To describe the termination of the slip event, we must instead account for the fact that, as velocity U becomes small enough, the exponential term in (10e) can no longer be ignored.

The full detail of the return of yield stress τ_c to its static value and the associated termination of the slip event are beyond our ability to capture analytically in this asymptotic solution. We show only how, increases in yield strength in the margins, where velocities are low due to the imposed boundary conditions, can lead to significant departures in velocity from the profile computed in (14) at late stages in the slip event. We expect that this initiates the termination of the slip event, and give an estimate for the time at which this should occur.

The role of low velocities in the margins: the main phase of the slip event

One possibility is that termination is initiated in the margins, where velocities are small due to the boundary condition (10f) and the exponential term in (10e) remains of $O(1)$. During the main part of a slip event, this leads to a larger amount of friction in a small boundary layer near the margin than is predicted in (13), but this only causes a small correction to the velocity field in (14). Let $\Lambda = \gamma\alpha \gg 1$. The solution (14) predicts that the exponential term $\exp(-\gamma\alpha|U|) = \exp(-\Lambda|U|)$ in (10e) is in fact of $O(1)$ within a distance $\sim 1/\Lambda$ of the margin, and therefore cannot be ignored in that region. This suggests a rescaling close to the margin; for the margin at $y = 0$, the relevant rescaling takes the form

$$Y = \Lambda y, \quad \tilde{U} = \Lambda U, \quad (16)$$

with an analogous theory possible to construct for the margin at $y = 2$. Under this rescaling, the equivalent of (11) and (12) becomes

$$\Lambda \frac{\partial^2 \tilde{U}}{\partial Y^2} = \beta \exp(-|\tilde{U}|) - \tau_c + 1 - \beta \quad (17)$$

$$\frac{\partial \tau_c}{\partial T} = \beta \exp(-|\tilde{U}|) - \tau_c + 1 - \beta \quad (18)$$

At leading order, the velocity field is unaffected by the velocity-dependent term on the right-hand side: Writing $\tilde{U} = \tilde{U}^{(0)} + \Lambda^{-1}\tilde{U}^{(1)} + O(\Lambda^{-2})$, the leading order solution that matches the far-field solution (14) for the bulk of the ice stream is

$$\tilde{U}^{(0)} = (\tau_{c0} - 1 + \beta)e^{-TY}. \quad (19)$$

The velocity-dependent term simply gives a first order correction that satisfies

$$\frac{\partial^2 \tilde{U}^{(1)}}{\partial X^2} = \beta \exp [(\tau_{c0} - 1 + \beta)e^{-TY}] - \tau_c^{(0)} + 1 - \beta, \quad (20a)$$

$$\frac{\partial \tau_c^{(0)}}{\partial T} = \beta \exp [(\tau_{c0} - 1 + \beta)e^{-TY}] - \tau_c^{(0)} + 1 - \beta. \quad (20b)$$

Although this defies a closed-form solution, it is clear that, during the main part of the slip event, the effect of the velocity-dependent term is confined to a boundary layer and remains small.

The role of low velocities in the margins: the late stages of the slip event

During the late stages of the slip event, as the velocity of the bulk of the ice stream drops, the correction to velocity U due to the exponential terms (10e) is no longer small compared with the velocity due to lateral shearing imposed by the bulk of the ice stream. This happens when $[\tau_{c0} - (1 - \beta)]e^{-T} \sim \Lambda^{-1/2}$, so when

$$T \sim \frac{1}{2} \log(\Lambda) + \log(\tau_{c0} - 1 + \beta). \quad (21)$$

At such late times, the boundary layer in which the velocity-dependent term in (10e) is of $O(1)$ has widened considerably, suggesting a further rescaling

$$\tilde{Y} = \Lambda^{1/2} y, \quad (22a)$$

$$\tilde{T} = T - \frac{1}{2} \log(\Lambda) - \log(\tau_{c0} - 1 + \beta) \quad (22b)$$

We also use the fact that, at this late time, the lateral shear stress τ is close to the profile required to maintain force balance with limiting dynamic friction as in (15):

$$\tau = (1 - \beta - f_n)(y - 1) + \Lambda^{-1/2} \tilde{\tau}. \quad (23)$$

Applying this to (10) with $f = f_n$ and still omitting the $O(\alpha^{-1})$ viscous term in the rheology, we have from (10) that

$$-\frac{\partial \tilde{\tau}}{\partial \tilde{Y}} - \tau_b + 1 - \beta = 0 \quad (24a)$$

$$\frac{\partial \tilde{\tau}}{\partial \tilde{T}} = -\frac{\partial \tilde{U}}{\partial \tilde{Y}} \quad (24b)$$

$$\tau_b = \tau_c \tilde{U} / |\tilde{U}| \quad \text{if } |\tilde{U}| > 0, \quad (24c)$$

$$|\tau_b| \leq \tau_c \quad \text{if } \tilde{U} = 0, \quad (24d)$$

$$\frac{\partial \tau_c}{\partial \tilde{T}} = \beta \exp(-|\tilde{U}|) + 1 - \beta - \tau_c, \quad (24e)$$

Matching with the main part of the slip event requires ‘initial’ conditions of the form $\tau_c \sim 1 - \beta$ as $\tilde{T} \rightarrow -\infty$, while matching with the interior of the ice stream

(which is still described by (10)) corresponds to $\tilde{\tau} \sim \exp(-\tilde{T})$ as $\tilde{Y} \rightarrow \infty$, and so $\partial\tilde{U}/\partial\tilde{Y} = -\partial\tilde{\tau}/\partial\tilde{T} = \exp(-\tilde{T})$. The no-slip boundary condition at the margin remains as $\tilde{U}(0, \tilde{T}) = 0$.

It should be clear that (24) allows for velocities \tilde{U} that can reach zero in the near-margin boundary layer due to the nonlinear term in (24e), while this was not possible during the earlier stages of the slip event, where the same term appears only at higher order in (20a). We therefore expect termination to be initiated at times $T \sim \log(\Lambda)/2$, although we are unable to state this with complete confidence.

While we cannot solve equations (24e) analytically, we can use the numerical model developed in this study to investigate the veracity of the asymptotic results, specifically the scaling of velocity (9) and termination time (equation 21, which is $\log(\gamma\alpha)/\alpha$ in dimensional terms). We specify driving stress directly in the model, as in Section 5.3 of the main text. The parameters we use are: $G=10^{10}$ Pa, $\nu=10^{11}$ Pa-hours, $W=100$ km, $H=1000$ m, $u_0=250$ m/a, $\tau_s=3$ kPa, $\tau_k=2$ kPa, and $\tau_d=-4$ kPa. T_b , the basal time constant, is varied, thus varying $\alpha = T_m/T_b$. T_b is given the values 0.025, 0.05, 0.1, 0.2, 0.4 hours, and so α varies from 25 to 400.

Fig. 1 plots the ratios of maximum velocity and α . (Values are normalized, so the first value is 1 by construction.) T_b is increasing from left to right, meaning α is decreasing. Δt_{term} , the time at which the slip event terminates, is not as clearly defined as maximum velocity. We choose to define this time based on the curvature of the velocity profile. Throughout most of the slip event, the profile is parabolic (and convex). When the slip event terminates this breaks down and part of the profile has positive second derivative, as seen from Fig. 5(a) of the main text. Thus we define Δt_{term} as the time (after the beginning of the event) at which u_{yy} takes on its maximum value (temporally and spatially). From inspection this metric agrees well with the point at which the slip terminates. FIG. 1 also plots the ratio of this value to $\log(\gamma\alpha)/\alpha$ (normalized as well).

The scaling of Δt_{term} seems to be accurate to within 10 %, subject to the assumption that our metric for termination time is correct. The scaling of velocity is less accurate; however, it is possible that at the larger values of α , the time step (.001 hours) was not small enough to capture the peak velocity at the beginning of the slip event.

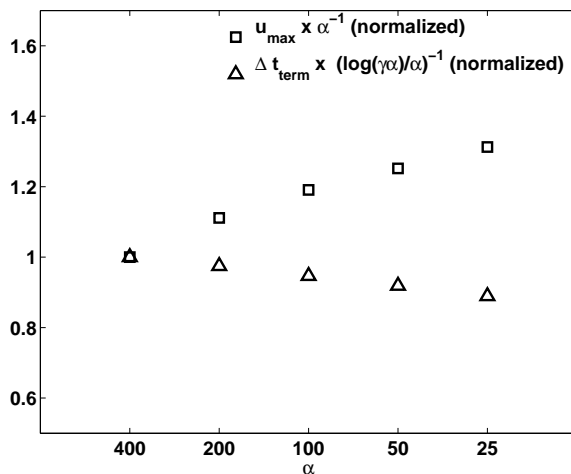


Figure 1: Ratio of maximum velocity to α , and of measured termination time to $\log(\gamma\alpha)/\alpha$. Values are normalized so that the leftmost value is 1.

1.3.3 The stick phase

The results above describe a single slip event starting at $t = t_n$ and lasting for a period of time we estimate at $\sim \log(\gamma\alpha)/\alpha$. The slip event is essentially described by (13)–(15); the analysis in §1.3.2 is intended only to indicate how the exponential decay in velocity described by (14) can eventually lead to complete shut down around time $T \sim \log(\Lambda)/2 = \log(\gamma\alpha)/2$. Assuming this to be the case, we can refine our assumptions on γ : we simply have to suppose that $\log(\gamma\alpha)/\alpha \ll 1$, so the complete shutdown (which permits basal friction to return to its static value) happens on time scales much faster than the Maxwell time. (23) then also shows that stress remains at its dynamic friction limit during this final termination of the slip event.

During the subsequent ‘stick’ phase of the stick-slip cycle, we can once more apply (8), but now with $u = 0$. In the limit $\alpha \gg 1$, we obtain a simple model for viscous

relaxation of the built-up elastic stress,

$$\frac{\partial \tau}{\partial y} - \tau_b + f = 0, \quad (25a)$$

$$\frac{\partial \tau}{\partial t} + \tau = 0, \quad (25b)$$

$$|\tau_b| \leq \tau_c, \quad (25c)$$

$$0 = 1 - \tau_c, \quad (25d)$$

with initial condition given by (15),

$$\lim_{t \rightarrow t_n^+} \tau(x, t) = (1 - \beta - f(t_n))(y - 1). \quad (26)$$

Stress now relaxes simply according to (25b), to give

$$\tau(x, t) = (1 - \beta - f(t_n)) \exp(-(t - t_n))(y - 1). \quad (27)$$

The basal shear stress required can be computed from (25a) throughout the stick phase. As the built-up elastic stress decays, basal shear stress has to rise, and we get

$$\tau_b = f(t) - (f(t_n) + \beta - 1) \exp(-(t - t_n)) \quad (28)$$

Meanwhile (25d) shows that the yield stress τ_c remains at its static value throughout the stick phase, owing to the fast relaxation time scale for friction. This justifies the statement above (14), that τ_{c0} is simply the static friction value of 1. From here it can be seen that, during the stick phase, the assumptions of the scaling for the stick phase duration in the main text (section 4.2) hold, and the (nondimensional) stick interval is given by

$$t_{n+1} - t_n = \log \left(\frac{f_0 - (1 - \beta)}{f_0 - 1} \right), \quad (29)$$

where t_{n+1} is the time of the next slip event. Note that if $\beta \ll 1$, that is, if static and kinetic yield stresses are very close, then

$$t_{n+1} - t_n \sim \frac{\beta}{f_0 - 1}. \quad (30)$$

Of large-scale interest is *not* the large values of velocity ($\sim 1/\alpha \times$ the viscous velocity scale) but the mean velocity averaged over a slip cycle, as this generates the ice flux

that changes ice geometry over long time scales. This average is easy to compute: we have

$$\bar{u}(y) = \frac{1}{t_{n+1} - t_n} \int_{t_n}^{t_{n+1}} u(y, t) dt,$$

where the integral has to include the slip event. In fact, the only non-zero contribution comes from the slip event. At leading order, applying the rescalings in §1.3.1 and using (14),

$$\int_{t_n}^{t_{n+1}} u(y, t) dt = \int_0^\infty U(y, T) dT = \int_0^\infty \frac{[\tau_{c0} - (1 - \beta)]e^{-T}}{2} (2y - y^2) dT = \frac{\beta(2y - y^2)}{2}$$

because it was shown that we can use $\tau_{c0} \equiv 1$. Then

$$\bar{u} = \frac{\beta(2y - y^2)}{2(t_{n+1} - t_n)}. \quad (31)$$

Fig. 2 compares this expression (with (29) for the interval length) with a velocity profile averaged over one stick-slip cycle for a given value of β . All parameters are as in Fig. 1, with $T_b=0.1$ hours, and values are dimensionalized. The profiles are almost coincident with each other.

The most interesting result applies when β is small, so the recurrence interval is given by (30). Then

$$\bar{u} \sim \frac{(f_0 - 1)(2y - y^2)}{2}, \quad (32)$$

or in dimensional variables,

$$\bar{u} \sim \frac{-(\tau_d + \tau_s)(Wy - y^2)}{2H\nu}. \quad (33)$$

This is in fact *exactly* the shearing profile one would obtain if there were no drop in friction at all and the ice stream behaved purely viscously. All that the slip events do in that case is to concentrate the flow into short time intervals, but they leave the time-averaged flux completely unchanged. For larger β , the recurrence interval $t_{n+1} - t_n$ changes slower than linearly with β , as opposed to a nearly-elastic rheology, where $t_{n+1} - t_n$ should be linear in β . Hence the mean discharge is increased somewhat above the purely viscous flow velocity in (33).

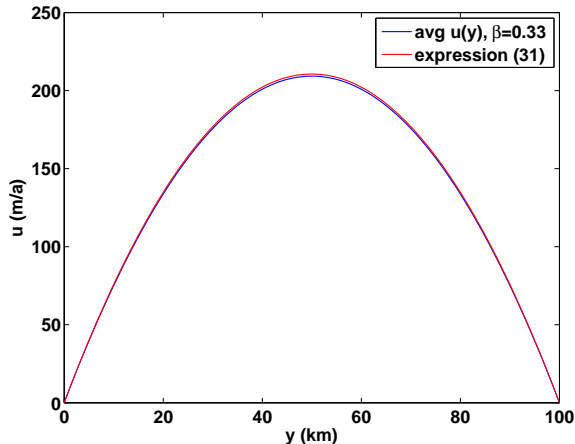


Figure 2: Time-averaged velocity profiles $\bar{u}(y)$ for different values of β .

1.4 Discussion

A relatively complete asymptotic solution can be given in closed form, which echoes many of the features of the analytical solution to the block slider model in the main paper, though some of the details are different. In particular, we analyze here the continuum model of the main paper, in which the duration of the slip event and details of the velocity field during the event are controlled by a friction model in which the yield stress of the bed asymptotically approaches dynamic friction over time, while inertial effects are negligible.

To obtain a mostly analytical solution, we have made several simplifications. Primarily, we omit the effect of upstream ice ‘pushing’ the stick-slip region from above, and we have also restricted the analysis to ice of constant viscosity. The advantage of the asymptotic solution is that, as with the block-slider model, various inferences can be drawn for relatively general parameter choices.

Two observations stand out from our results: Firstly, in order to generate stick-slip events it suffices to have a velocity-weakening friction law coupled with a viscoelastic ice rheology. The stick-slip motion need not be tied to a tidal cycle, but can be generated purely by the viscous relaxation of stresses in the ice, as explained in the main text. The length of a stick-slip cycle under these ‘unforced’ conditions is then proportional to the Maxwell time. The second observation is that, although

instantaneous velocities during the slip event can be large, the time-averaged velocity field remains similar to that computed from a purely viscous model in the absence of velocity-weakening friction. In fact, in our model, slip velocities scale relative to purely viscous velocities as the ratio of Maxwell time to bed adjustment $1/\alpha = T_M/T_b$, and can be made larger by choosing a shorter bed adjustment time scale. However, longer-time ice dynamics (i.e., relevant to the evolution of ice thickness) will only see the time-averaged velocity, and the occurrence of stick-slip cycles may not signal any significant change in the latter relative to purely viscous flow in the absence of velocity-weakening friction. If true, this would imply that stick-slip events are of minor consequence for the large-scale dynamics of ice sheets, unless the occurrence of velocity-weakening friction is a symptom of other, more fundamentally significant changes at the ice stream bed.

2 Rate and state treatment of basal stress

The basal sliding law implemented in our model (main text, equations 9-10) is intended as a phenomenological description of bed strength evolution, one in which the functional form and the parameters are based on observed time and length scales associated with slip events. It is not intended to arise from any specific glaciological process. In non-glaciological contexts, however, studies of stick-slip have made use of rate-and-state models of friction (e.g., *Ruina*, 1983; *Segall and Rice*, 1995; *Rubin and Ampuero*, 2005). In these models of bed friction, frictional resistance depends on both sliding velocity and a “state variable” (often called θ), which serves as a macroscopic description of microscopic asperities at the sliding interface, and gives friction some degree of “memory”. There are different types of rate-and-state laws, particularly concerning the evolution of θ . *Rubin and Ampuero* (2005) identifies both a “slip law” and an “aging law”, where the latter is so named because θ increases when sliding is negligible, as opposed to the slip law.

In the following, the bed model from the main text (equations 9-10) is referred to as the “phenomenological” model, to distinguish from rate-and-state models. It can be argued that rate-and-state friction models are themselves phenomenological, arising from attempts to mathematically explain frictional behavior in lab experiments; however, we reserve the term here to reflect our attempt to reproduce the behavior observed from GPS measurements of Whillans Ice Plain.

2.1 Connection between phenomenological stress model and “Slip” rate and state

Though not intended as a rate-and-state formulation, it can be shown that our treatment is very similar to the “slip” law as presented in *Rubin and Ampuero (2005)*. In particular, if the explicit velocity-dependence of stress is set to zero, then the two laws are nearly equivalent, save for the fact that the slip timescale T_b is a constant in our treatment, whereas in the rate-and-state law it is proportional to sliding velocity. We demonstrate this below.

In rate and state formulations the equation for frictional strength τ can be written as

$$\tau = \sigma \left(f^* + a \ln \frac{u}{u_0} + b \ln \frac{u_0 \theta}{D_c} \right), \quad (34)$$

where σ is normal stress, and f^* , a and b are parameters. D_c is often cited as a characteristic slip distance. The quantity θ , with a “slip” law, evolves according to

$$\dot{\theta} = -\frac{u\theta}{D_c} \ln \left(\frac{u\theta}{D_c} \right). \quad (35)$$

If $b > a$, the friction law is rate-weakening. We assume that $a = 0$; this is equivalent to saying that friction does not depend on velocity; this is true of a plastic friction law. In this case, for a given u , we can find a steady-state θ :

$$\theta_{ss} = \frac{D_c}{u}, \quad (36)$$

i.e. a value of θ for which $\dot{\theta}$ is zero. This then gives a “steady-state” friction τ_{ss} which depends only on u :

$$\tau_{ss}(u) = \sigma \left(f^* - b \ln \frac{u}{u_0} \right); \quad \tau - \tau_{ss}(u) = \sigma b \ln \frac{u\theta}{D_c}. \quad (37)$$

If we differentiate (34) by t , we get

$$\dot{\tau} = \sigma b \frac{\dot{\theta}}{\theta} = -\sigma b \frac{u}{D_c} \ln \left(\frac{u\theta}{D_c} \right) = -\frac{u}{D_c} (\tau - \tau_{ss}(u)). \quad (38)$$

This is very similar to our phenomenological bed strength model, with yield stress playing the role of τ . The negative log behavior of $\tau_{ss}(u)$ differs from the exponential decay of our phenomenological model, but qualitatively the dependence on u is

similar. An important difference, however, is that in the phenomenological model ($\tau - \tau_{ss}(u)$) is divided by a characteristic slip timescale T_b . The fraction u/D_c multiplier can be seen as an inverse timescale, but one which varies with velocity u . This may have an impact on the dynamics of stick-slip, but otherwise the bed stress models are very similar.

2.2 Implementation of “aging” rate and state in the model

The above discussion shows how our phenomenological basal treatment is very similar to a rate-and-state “slip” law. In these types of models, bed strength does not increase when sliding velocity is close to zero. However, another type of rate-and-state formulation, an “aging” type (*Rubin and Ampuero, 2005*), allows for slow strengthening during stagnancy. In this bed model, (35) is replaced by

$$\dot{\theta} = 1 - \left(\frac{u\theta}{D_c} \right). \quad (39)$$

Implementation of the rate-and-state model in our numerical model is very straightforward. τ_b^ε , which appears in equation (A3) of the main text, is replaced by τ from (34) and θ is evolved according to (39). Since we do not consider fluctuations in normal stress, (34) is rewritten

$$\tau = \hat{F} + \hat{A} \ln \frac{u}{u_0} + \hat{B} \ln \frac{u_0 \theta}{D_c}. \quad (40)$$

We do not know of any previous published studies of stick-slip of an ice stream with rate-and-state friction, and again have little else to constrain the parameters (\hat{F} , \hat{A} , \hat{B} , u_0 , and D_c) other than scales of observed behavior. An advantage of the rate-and-state formulation is that we do not need to include an inertial damping term, as discussed in the Appendix of the main text, as basal stress is no longer decoupled from velocity during the slip event.

Fig. 3(a) shows u_{max} over time where aging rate-state friction has been implemented. Aside from bed friction parameters, the model parameters are the same as in the simulation of Fig. 3(a) of the main text, i.e. it is a stress-driven simulation, not a push-driven one. The parameters of the rate-state formulation are as follows: $\hat{A} = 3$ kPa, $\hat{B} = 75$ Pa, $\hat{F} = 2$ kPa, $u_0 = 10$ m/a, and $D_c = 0.2$ mm. As stated above,

the parameters were in part chosen based on knowledge of general scales (i.e. bed strength ~ 1 kPa, u_0 is on the order of the velocity in “stick” phase). D_c was then chosen such that the observed slip timescale was 10-30 minutes.

A similar pattern of behavior is seen to stick-slip with the phenomenological bed model. Certain other properties hold as well, at least in a qualitative sense. Varying D_c within a narrow range can change the details of a slip event dramatically, as seen in Fig. 3(c). Still, the time-averaged velocity changes relatively little (Fig. 3(b)). Note that the average velocity is larger than that of the phenomenological model (main text, Fig. 5(b)); this is simply because the sliding parameterization is fundamentally different. Also, it is difficult to isolate the slip timescale and control it (as opposed to the phenomenological model, in which T_b can be modified directly). Still, these results suggest that the notion of the average velocity being insensitive to some aspects of the slip phase might not be limited to the phenomenological bed model. A further comparison between the aging rate-state bed model and the phenomenological model is made by observing how tides modify the frequency spectrum, and how they affect time-averaged velocity, as was done for the phenomenological model in the main text. The experiments with the rate-state model are shown in Fig.4.

Fig. 4(a) shows the effects on the frequency spectrum. As in the above experiments, the parameters differ from those in Fig. 10 of the main text only in the basal stress formulation. The rate-state parameters are as above. As with the phenomenological model, there is a pattern of regularly-spaced peaks for the non-tidally forced case, indicating an unforced frequency of ~ 4.6 hours. In contrast to the phenomenological model, though, the peaks are less uniform and slightly wider at higher frequencies, and there is some irregular noise at higher harmonics, although it is minimal. A small forcing ($\eta_{tide} = 0.1m$) with period 12h, makes the spectrum becomes quite noisy at frequencies of less than ~ 40 minutes. Still, the first few peaks remain intact, indicating a still-strong presence of the unforced frequency. The forcing frequency is not detectable. With a strong forcing, the forcing frequency can be seen, although it is weak. The first peak of the unforced spectrum remains, indicating the persistence of the 4.6-hour cycle, although the spectrum is noticeably different from the unforced spectrum, even at lower harmonics.

Fig. 4(b) shows results from the experiment shown in Fig. 11 from the main text, with aging rate-state instead of the phenomenological model. Results are shown for the stress-driven model only. As can be seen, the time-averaged velocities are not affected by the presence of tides, even though tidal forcing modifies the frequency

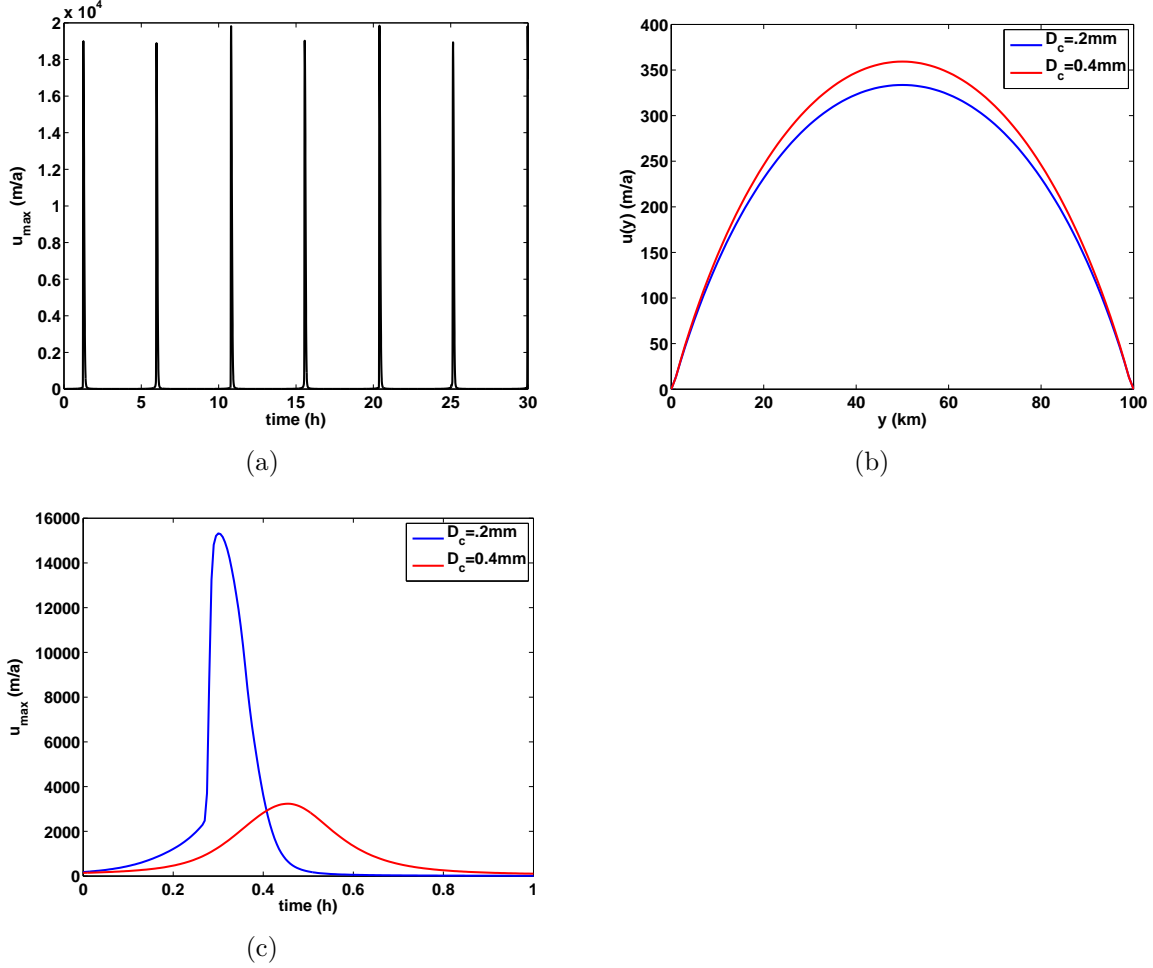


Figure 3: (a) Slip events with aging rate-state law. Parameters are as in Fig. 3(a) of the main text, with the exception of bed parameters, which are given above. (b) Time-averaged velocity profiles for two different values of characteristic slip distance D_c ; other parameters are as in (a). (c) Individual slip events with differing values of D_c .

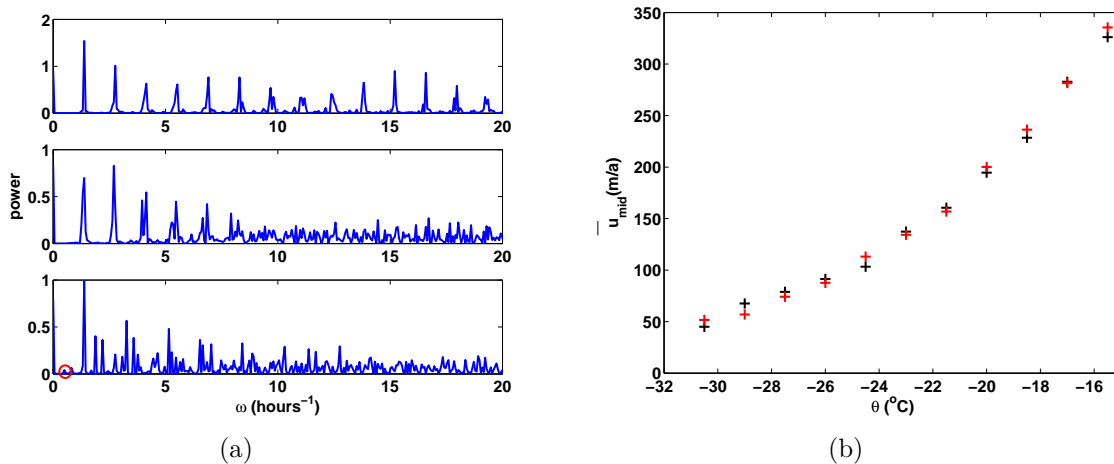


Figure 4: (a) Spectra of u_{max} with different levels of tidal forcing, as in Fig. 10 of the main text but with aging rate-and-state friction. (b) Time-averaged (centerline) velocities as in Fig. 11 of the main text (red→tidally forced). Only stress-driven results are shown.

spectrum greatly.

The result that average velocities are unchanged is surprising, even more so than in the phenomenological bed model case. This is because in the phenomenological model, the “strong” and “weak” bed states are fixed, and therefore slip distances are fixed for a given simulation. This is not the case for an aging rate-state friction model, as tidal forcing leads to variable-length stick intervals, and the “aging” component of the rate-state formulation leads to variations in the strong state of the bed. Owing to the log-dependence of the friction on the θ , however, this effect may be very weak. In any event, the result in the main text is recovered using an alternative friction formulation. These experiments demonstrate that the results of the main text are reproduced qualitatively using a different model for bed friction. This does not mean that the results are unequivocally correct; but given the uncertainty regarding the mechanism of rate-weakening of the ice-bed interface on Whillans Ice Plain, it is important to demonstrate that the results of the study do not depend strongly on a somewhat arbitrary choice of the representation of interface physics. The purpose of these experiments is to show that this is not the case.

References

- Rubin, A. M., and J. P. Ampuero, Earthquake nucleation on (aging) rate and state faults, *Journal of Geophysical Research-Solid Earth and Planets*, 110, B11,312, doi:10.1029/2005JB003686, 2005.
- Ruina, A., Slip instability and state variable friction laws, *Journal of Geophysical Research*, 88(B12), doi:10.1029/JB088iB12p10359, 1983.
- Segall, P., and J. R. Rice, Dilatancy, compaction, and slip instability of a fluid infiltrated fault, *Journal of Geophysical Research*, 100(B11), doi:10.1029/95JB02403, 1995.